Heterogeneous core-mantle boundary heat flux in thermo-chemical core convection

Veit Lüschow

May 12, 2016

Contents

Abstract

Thermal coupling between convection in Earth's mantle and core was proposed to explain asymmetric features of the geomagnetic field during the history of the Earth. The coupling is caused by laterally varying heat transport from the core to the mantle, induced by lateral temperature gradients in the lower-most mantle. Clues for the temperature gradients were found by seismic tomography.

This numerical study aims to explore the influence of these non-uniform boundary conditions, as compared to uniform heat flux and isothermal boundary conditions on thermo-chemical core convection and some distinct dynamo properties.

In our model the heat flux pattern is modeled by a single spherical harmonic of degree and order 2. This setting conserves equatorial symmetry, but imposes azimuthal heat flux gradients.

Today, convection in the Earth's core is assumed to be driven predominantly by a combination of thermal and compositional buoyancy sources located at the inner-core boundary. Thermal and compositional diffusivities differ by orders of magnitude. The resulting differences in the dynamical behavior of the two components demand an approach with distinct transport equations and boundary conditions for temperature and chemical concentration. Simulations for five different ratios of thermal and chemical driving are made.

We observe that fixed flux conditions promote larger flow scales and an increase of mean kinetic energy densities. The imposed flux pattern locks the outer core flow to the mantle and therefore breaks its azimuthal symmetry, even for relatively low thermal forcing ratios of 20 %. Despite of the symmetry breaking, stable and dipolar dynamos can be maintained due to the partly chemical forcing with its uniform boundary conditions. Additionally, the chemical component partly adopts to the geometry of the heat flux pattern because advective transport of concentration is more effective in regions of increased heat flux.

1 Introduction and Motivation

1.1 A thermo-chemical approach to dynamo modeling

1.2 Why use heterogeneous heat flux boundary conditions?

2 Modeling core convection and dynamo action

Rotating convection and dynamo action in Earth's core is a topic that has been explored by many authors (REFS ???). There exist various ideas of how to formulate a set of equations that depicts all relevant physical processes and that is still as simple and therefore numerically economical as possible. Computation time is the limiting factor when it comes to the question how realistic models of the inner core can be. The gap between the relevant physical parameters expected for the Earth and the param-

eters that are in range of numerical modeling is still big. It cannot be expected that this gap will be closed only with the help of the increasing computational resources that will become available within the next years. Alternatives to waiting for larger computers that allow to explore earth-like parameters have to be found. Asymptotic models are one possibility already revealing promising results (REFS ???).
A question that is closely related to the numerical costs and therefore to the accessible parameter range is the choice of the geometry. Most models are either Cartesian with periodic boundary conditions or spherical shell models. The latter are of course more realistic for the Earth but numerically more costly and therefore even less earth-like with regard to computational feasible parameters. In this work, a spherical model is used in order to be as earth-like as possible in a geometrical way. As a trade-off, parameter regimes in which Cartesian models could advance, are unreachable here.
We model the electrically conducting liquid outer core. It is enclosed by the inner-core boundary (ICB) at the bottom and the core-mantle boundary (CMB) at the top. Convection is driven by destabilizing thermal and compositional gradients across the sphere. For the compositional component, fixed chemical concentrations at the ICB and the CMB are imposed (Derichlet boundary condition). The thermal forcing is maintained by introducing a fixed in - and out flux of heat (Neumann boundary condition). The heat flux at the CMB is laterally heterogeneous, i.e., there exist regions of higher and lower heat flux than lateral average. The inner core and mantle are assumed to be insulating and therefore have no influence on the evolution of magnetic fields.
In the following all relevant equations are introduced. There exist numerous detailed derivations so that this description will be held relatively short (REFS ???).

2.1 Frame of reference

The liquid outer core (LOC) is modeled in a spherical shell with an inner radius R_i and an outer radius R_o. It is bounded by the ICB at the bottom the CMB at the top. The shell thickness is chosen according to what is expected for today's state of the Earth and defined over the ratio between R_i and r_o: $a = \mathrm{R}_i \ / \ \mathrm{R}_i = 0.35$.
The LOC is constantly rotating about the z-axis of a Cartesian system. The angular velocity Ω is invariant in time. The effect of the rotation on the frame of reference will be discussed when it comes to the equation of motion. In the course of this study,it is quite nearby to chose spherical coordinates (???).

2.2 Equation of continuity

Per definition, the mass $\mathcal{M}$ of a material volume $\mathcal{V}(t)$ with a density ρ, moving with a velocity $\boldsymbol{u}(\boldsymbol{r}, t)$ in a fluid is conserved:

$$\frac{d\mathcal{M}(\mathcal{V})}{dt} = \frac{d}{dt} \int_{\mathcal{V}(t)} \rho(\boldsymbol{r}, t) d^3 r = 0 \tag{1}$$

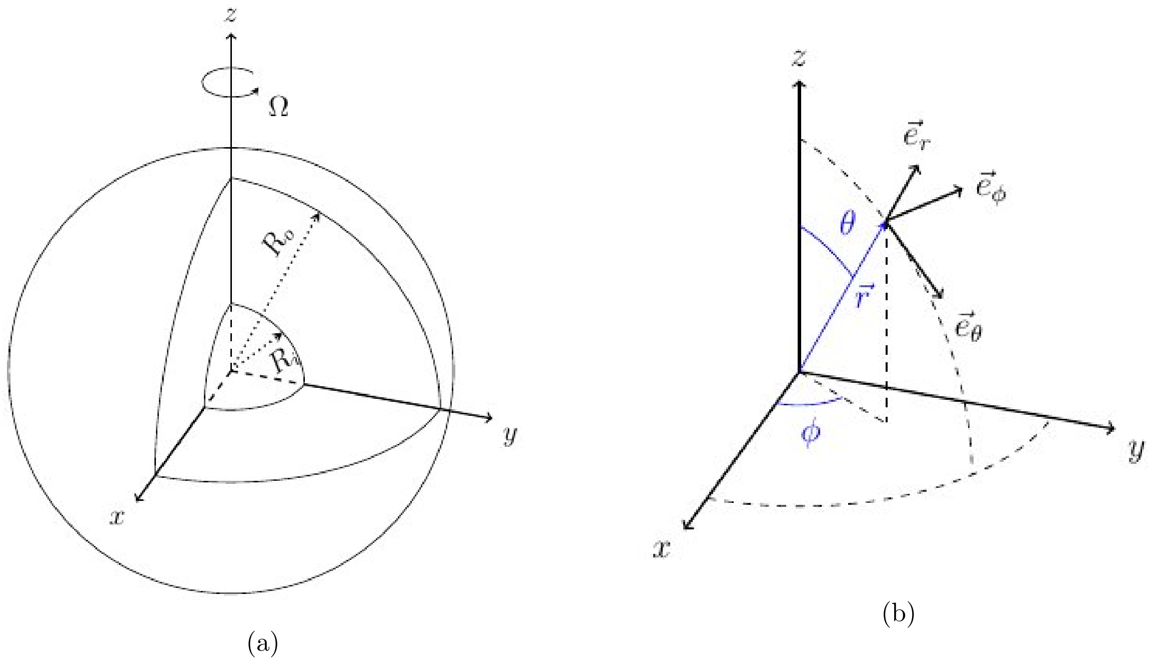

Figure 1: (a) (REFS ???) Sketch of the liquid outer core. It is bounded by the two spheres of radii R_i and R_o. The rotation axis is the cartesian z-axis. (b) This work uses spherical coordinates with unit vectors $\boldsymbol{e}_r$, $\boldsymbol{e}_\Phi$ and $\boldsymbol{e}_\vartheta$

Using Reynold's Transport Theorem (Appendix ???) and then applying Gauss's Theorem, this yields

$$\int_{\mathcal{V}(t)} \frac{\partial \rho}{\partial t} d^3 r + \oint_{\partial \mathcal{V}(t)} \rho \boldsymbol{u} \cdot \boldsymbol{ds} = \int_{\mathcal{V}(t)} \left[\frac{\partial \rho}{\partial t} + \boldsymbol{\nabla} \cdot (\rho \boldsymbol{u}) \right] d^3 r = 0. \tag{2}$$

Since this has to hold for all possible material volumes $\mathcal{V}$, one gets

$$\frac{\partial \rho}{\partial t} + \boldsymbol{\nabla} \cdot (\rho \boldsymbol{u}) = 0, \tag{3}$$

the general form of the equation of continuity. The introduction of the *material derivative* $\frac{D}{Dt} = \frac{\partial}{\partial t} + \boldsymbol{u} \cdot \boldsymbol{\nabla}$ suggests another useful formulation:

$$\frac{\partial \rho}{\partial t} + \rho \boldsymbol{\nabla} \cdot \boldsymbol{u} + \boldsymbol{u} \cdot \boldsymbol{\nabla} \rho = \frac{D\rho}{Dt} + \rho \boldsymbol{\nabla} \cdot \boldsymbol{u} = 0. \tag{4}$$

2.3 Equation of momentum

In an inertial, non-rotating frame of reference, the change of momentum of a material volume $\mathcal{V}$ can be written as

$$\begin{aligned}\frac{d}{dt}\int_{\mathcal{V}(t)}(\rho u_j)d^3r &= \int_{\mathcal{V}(t)}\left[\frac{\partial(\rho u_j)}{\partial t}+\frac{\partial}{\partial x_i}(\rho u_j)u_i\right]d^3r \\ &= \int_{\mathcal{V}(t)}\left[\rho\frac{\partial u_j}{\partial t}+u_j\frac{\partial \rho}{\partial t}+\rho u_j\frac{\partial u_i}{\partial x_i}+u_i\rho\frac{\partial u_j}{\partial x_i}+u_iu_j\frac{\partial \rho}{\partial x_i}\right]d^3r \\ &= \int_{\mathcal{V}(t)}\left[u_j\left(\frac{\partial \rho}{\partial t}+\rho\boldsymbol{\nabla}\cdot\boldsymbol{u}+\boldsymbol{u}\cdot\boldsymbol{\nabla}\rho\right)+\rho\left(\frac{\partial u_j}{\partial t}+\boldsymbol{u}\cdot\nabla u_j\right)\right]d^3r \\ &= \int_{\mathcal{V}(t)}\rho\frac{Du_j}{Dt}d^3r.\end{aligned}$$

Change of momentum can happen through either *volume forces* $\boldsymbol{f}$ or *surface forces* $\boldsymbol{t}$:

$$\int_{\mathcal{V}}\rho\frac{D\boldsymbol{u}}{Dt}d^3r = \int_{\mathcal{V}}\boldsymbol{f}d^3r + \oint_{\partial\mathcal{V}}\boldsymbol{t}ds \tag{5}$$

If a frame of reference is rotating - as in this case - it is no longer an inertial system and therefore pseudo forces have to be expected. Under the assumption of a constant rotation with the angular velocity Ω and a fixed rotation axis parallel to the Cartesian z-axis, the change of a quantity $\boldsymbol{P}$ in the rotating frame of reference and its change in the non-rotating inertial frame relate as

$$\left(\frac{d\boldsymbol{P}}{dt}\right)_F = \left(\frac{d\boldsymbol{P}}{dt}\right)_R + \boldsymbol{\Omega}\times\boldsymbol{P}, \tag{6}$$

where the subscripts F and R indicate the *fixed* and the *rotating* frame. Applying rule (6) twice to a position vector $\boldsymbol{r}$ yields

$$\boldsymbol{a}_F = \boldsymbol{a}_R + 2\boldsymbol{\Omega}\times\boldsymbol{u}_R + \boldsymbol{\Omega}\times(\boldsymbol{\Omega}\times\boldsymbol{r}) \tag{7}$$

for accelerations $\boldsymbol{a}$. $2\boldsymbol{\Omega}\times\boldsymbol{u}_R$ is the Coriolis force and $\boldsymbol{\Omega}\times(\boldsymbol{\Omega}\times\boldsymbol{r})$ the centripetal force.
With the help of (7), $\frac{D\boldsymbol{u}}{Dt}$ can be transferred from the inertial frame to the frame of reference:

$$\frac{D\boldsymbol{u}_F}{Dt} = \frac{D\boldsymbol{u}_R}{Dt} + 2\boldsymbol{\Omega}\times\boldsymbol{u}_R + \boldsymbol{\Omega}\times(\boldsymbol{\Omega}\times\boldsymbol{r}) \tag{8}$$

From now on, the subscripts F and R will be cut and all quantities will be measured in the rotating frame. With (8), (5) changes to

$$\int_{\mathcal{V}}\rho\frac{D\boldsymbol{u}}{Dt}d^3r = \int_{\mathcal{V}}\boldsymbol{f}d^3r + \oint_{\partial\mathcal{V}}\boldsymbol{t}ds - \int_{\mathcal{V}}\rho\left(2\boldsymbol{\Omega}\times\boldsymbol{u}_R + \boldsymbol{\Omega}\times(\boldsymbol{\Omega}\times\boldsymbol{r})\right)d^3r. \tag{9}$$

Another pseudo force that generally appears in rotating systems is the *Poincaré force.* Precession driven flows are the most prominent example from geophysics where it plays

a dominant role (Tilgner, 2007).
The *Cauchy Theorem* relates the surface forces $\boldsymbol{t}$ to the stress tensor $\underline{\tau}$ linearly via $\boldsymbol{t} = \underline{\tau} \cdot \boldsymbol{n}$, where $\boldsymbol{n}$ is the normal vector. The surface term in (9) can thus be transformed to

$$\oint_{\partial\mathcal{V}} \boldsymbol{t} ds = \int_{\mathcal{V}} \boldsymbol{\nabla} \cdot \underline{\tau} d^3 r, \tag{10}$$

where $\boldsymbol{\nabla} \cdot \underline{\tau} = -\boldsymbol{\nabla} p + \mu \boldsymbol{\nabla}^2 \boldsymbol{u}$ will be used as a reasonable simplification in the context of the Boussinesq approximation (see section 2.7). This expression of $\boldsymbol{\nabla} \cdot \underline{\tau}$ is valid for Newtonian fluids and it is based on the assumption of a solenoidal velocity field ($\boldsymbol{\nabla} \cdot \boldsymbol{u} = 0$) and a homogeneous dynamic viscosity μ throughout the fluid.
The body forces $\boldsymbol{f}$ are the *buoyancy force* $\boldsymbol{f}_g = \boldsymbol{g}\rho$ and the *Lorentz force* $\boldsymbol{f}_l = \boldsymbol{j} \times \boldsymbol{B}$. The latter will be discussed in section 2.4.

In the following, the gravitational field $\boldsymbol{g}$ will be discussed in more detail.As mentioned before, the system underlies an asymmetric heat flux at the CMB. This results in an asymmetric temperature field for which the penetration depth of the temperature perturbation to a spherical symmetric solution depends on the amplitude of the heat flux heterogeneity. Following the linear equation of state from the Boussinesq approximation (see section 2.7), this results in a density variation proportional to the temperature variation: $\delta\bar{\rho} \sim \delta\bar{T}$.

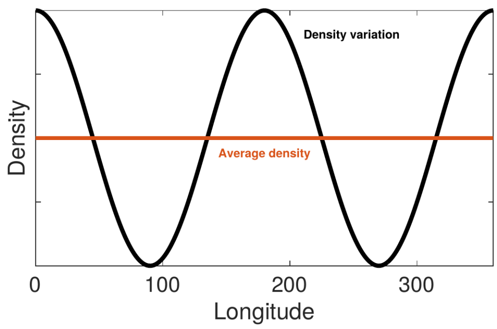

Figure 2: Sketch of the density along the equator, near the CMB. The deviation (black) from the average density (red) results from the asymmetric heat flux at the CMB which has a asymmetric temperature field as a consequence.

The total density can be split into one spherical symmetric part $\bar{\rho}(r)$ that only depends on the radial level r and the density variation $\delta\bar{\rho}(r, \vartheta, \varphi)$:

$$\rho(r, \vartheta, \varphi) = \bar{\rho}(r) + \delta\bar{\rho}(r, \vartheta, \varphi). \tag{11}$$

In case of a heat flux pattern proportional to the spherical harmonic $\mathcal{Y}_2^2$, the dependence of $\delta\bar{\rho}$ on φ is π-periodic (see Figure 2) so that it can be expressed by the product $\delta\bar{\rho}(r, \vartheta, \varphi) = \mathcal{C}(r, \vartheta) \cdot cos(2\varphi)$. $\mathcal{C}$ is only a function of r and ϑ.
Gauss's gravity law (Blakely, 1996) states

$$\boldsymbol{\nabla} \cdot \boldsymbol{g} = -4\pi G \rho(r, \vartheta, \varphi). \tag{12}$$

Integration over a sphere of radius r and application of Gauss's theorem yields

$$\int\limits_{\mathcal{V}(r)} \boldsymbol{\nabla} \cdot \boldsymbol{g} dV = \int\limits_0^{\pi}\int\limits_0^{2\pi} r^2 sin(\vartheta) d\vartheta d\varphi \boldsymbol{g} \cdot \boldsymbol{e}_r = -4\pi G \int\limits_0^{r}\int\limits_0^{\pi}\int\limits_0^{2\pi} sin(\vartheta) r'^2 \rho(r,\vartheta,\varphi) dr' d\vartheta d\varphi$$

$$= -4\pi G \int\limits_0^{r}\int\limits_0^{\pi}\int\limits_0^{2\pi} sin(\vartheta) r'^2 [\bar{\rho}(r') + \delta\bar{\rho}(r',\vartheta,\varphi)] dr' d\vartheta d\varphi$$

$$= -8\pi^2 G \int\limits_0^{r} \bar{\rho}(r') dr' - 4\pi G \int\limits_0^{r}\int\limits_0^{\pi} sin(\vartheta) r'^2 \mathcal{C}(r',\vartheta) \left(\int\limits_0^{2\pi} cos(2\varphi) d\varphi \right) dr' d\vartheta$$

$$= -8\pi^2 G \int\limits_0^{r} \bar{\rho}(r') dr'$$

Because the integration of $\delta\bar{\rho}(r',\vartheta,\varphi)$ over φ drops out for every value of r and ϑ, $\boldsymbol{g}$ can be expressed by

$$\boldsymbol{g}(\boldsymbol{r}) = -\frac{4\pi G}{r^2} \int_0^r \bar{\rho}(r') r'^2 dr \boldsymbol{e}_r \tag{13}$$

and it is worth noticing that $\boldsymbol{g}$ has the same form as in the spherical symmetric case.

2.4 Maxwell equations, Lorentz force and induction equation

The liquid outer core consists of a metallic and therefore conducting fluid. Electric currents may evolve, create magnetic fields and these again may generate currents and influence the flow field. The induction equation is a transport equation for a magnetic fields $\boldsymbol{B}$ 'hosted' by a fluid moving with a velocity $\boldsymbol{u}$. The Lorentz force characterizes the influence of the magnetic field on the flow field, whereas the Maxwell equations describe how electric and magnetic fields interact through charges and currents. They form a basis for the 'magnetic part' of Magnetohydrodynamics (MHD).
In the scope of core convection, a reduced form of the Maxwell equations (Pre-Maxwell equations) suffices (REF Davidson ???):

$$\boldsymbol{\nabla} \times \boldsymbol{B} = \mu_0 \boldsymbol{j} \qquad \text{(Ampère's law)} \tag{14a}$$

$$\boldsymbol{\nabla} \cdot \boldsymbol{j} = 0 \qquad \text{(Charge conservation)} \tag{14b}$$

$$\boldsymbol{\nabla} \times \boldsymbol{E} = -\frac{\partial \boldsymbol{B}}{\partial t} \qquad \text{(Faraday's law)} \tag{14c}$$

$$\boldsymbol{\nabla} \cdot \boldsymbol{B} = 0 \qquad \text{(No magnetic monopoles)} \tag{14d}$$

Additionally, an extended version of *Ohm's law* for moving conductors

$$\boldsymbol{j} = \sigma(\boldsymbol{E} + \boldsymbol{u} \times \boldsymbol{B}) \tag{15}$$

and an expression for the *Lorentz force*

$$\boldsymbol{f}_l = \boldsymbol{j} \times \boldsymbol{B} = \frac{1}{\mu_0}(\boldsymbol{\nabla} \times \boldsymbol{B} \times \boldsymbol{B}) \tag{16}$$

are needed. $\boldsymbol{E}$ describes the electric field, $\boldsymbol{j}$ the current density, μ_0 the vacuum permeability and σ the conductivity of the fluid.
The *induction equation*, a transport equation for the magnetic field, can be derived using (14c), (15) and the solenoidal character of $\boldsymbol{B}$ (14d) and $\boldsymbol{u}$:

$$\frac{\partial \boldsymbol{B}}{\partial t} = \boldsymbol{\nabla}(\boldsymbol{u} \times \boldsymbol{B}) + \eta \boldsymbol{\nabla}^2 \boldsymbol{B}, \tag{17}$$

where $\eta = \frac{1}{\sigma \mu_0}$ is the magnetic diffusivity.

2.5 Conservation of energy

The conservation of internal energy in a fluid reads

$$\rho \frac{De}{Dt} = -\boldsymbol{\nabla} \cdot \boldsymbol{q}_{\mathrm{T}} - p(\boldsymbol{\nabla} \cdot \boldsymbol{u}) + \Phi, \tag{18}$$

where the internal energy per unit mass is described by e. It can be changed by either *volume compression* $-p(\boldsymbol{\nabla} \cdot \boldsymbol{u})$, *viscous dissipation* Φ or a *heat flux* $\boldsymbol{q}_{\mathrm{T}}$ through the fluid surface. In the context of the Boussinesq approximation (section 2.7), viscous dissipation Φ is negligible and $\boldsymbol{\nabla} \cdot \boldsymbol{u} = 0$. Furthermore, using the *Fourier law* $\boldsymbol{q}_{\mathrm{T}} = -k_{\mathrm{T}} \boldsymbol{\nabla} T$ and the *perfect gas* approximation $e = c_{\mathrm{P}} T$, (18) can be transformed to

$$\frac{DT}{Dt} = \kappa_{\mathrm{T}} \boldsymbol{\nabla}^2 T. \tag{19}$$

Here, $\kappa_{\mathrm{T}} = \frac{k}{c_{\mathrm{P}} \rho}$ is the thermal diffusivity and T the fluid temperature. Internal sources of e in the liquid outer core are completely omitted in this study.
The derivation of equation (19) was adopted from Kundu and Cohen (2008).

2.6 Conservation of the light component

The light component is released at the ICB as the inner core slowly crystallizes. It serves as an additional source of buoyancy. In this model, the light component per unit mass, C, can only change by a flux $\boldsymbol{q}_{\mathrm{C}}$through the surface of the fluid. According to the equation for the conservation of the internal energy in section 2.5,

$$\rho \frac{DC}{Dt} = -\boldsymbol{\nabla} \cdot \boldsymbol{q}_{\mathrm{C}}$$

can be transformed to

$$\frac{DC}{Dt} = \kappa_{\mathrm{C}} \boldsymbol{\nabla}^2 C, \tag{20}$$

using $\boldsymbol{q}_{\mathrm{C}} = -k_{\mathrm{C}} \boldsymbol{\nabla} C$ and introducing $\kappa_{\mathrm{C}} = \frac{k_{\mathrm{C}}}{\rho}$.

2.7 The Boussinesq approximation

2.8 Nondimensional equations

2.9 CMB - heat flux pattern

A heat flux balance between the inner and the outer core boundary is imposed. The total influx at the ICB Q_i equals the total outflux Q_o at the CMB:

$$-\mathrm{Q}_i = \mathrm{Q}_o \tag{21}$$

$$\Leftrightarrow \int\limits_{\Sigma_{\mathrm{icb}}} \kappa \nabla T\big|_{\mathrm{icb}} \cdot \boldsymbol{e}_r dS = \int\limits_{\Sigma_{\mathrm{cmb}}} \kappa \nabla T\big|_{\mathrm{cmb}} \cdot \boldsymbol{e}_r dS \tag{22}$$

$$\Leftrightarrow \int\limits_{\Sigma_{\mathrm{icb}}} \frac{\partial T}{\partial r}\bigg|_{\mathrm{icb}} dS = \int\limits_{\Sigma_{\mathrm{cmb}}} \frac{\partial T}{\partial r}\bigg|_{\mathrm{cmb}} dS \tag{23}$$

For the spectral decomposition it is important to know, that only the 0th order spherical harmonic $\mathcal{Y}_0^0$ yields values $\neq 0$ when integrated over a closed surface Σ:

$$\int\limits_{\Sigma} \frac{\partial T}{\partial r} dS = \int\limits_{\Sigma} \left(\frac{\partial T}{\partial r}\right)_0^0 \mathcal{Y}_0^0 dS \tag{24}$$

with $\left(\frac{\partial T}{\partial r}\right)_0^0$ being the spectral coefficient of degree and order 0.

$$\int\limits_{\Sigma_{\mathrm{icb}}} \left(\frac{\partial T}{\partial r}\right)_0^0\bigg|_{\mathrm{icb}} \mathcal{Y}_0^0 dS = \int\limits_{\Sigma_{\mathrm{cmb}}} \left(\frac{\partial T}{\partial r}\right)_0^0\bigg|_{\mathrm{cmb}} \mathcal{Y}_0^0 dS \tag{25}$$

$$\Leftrightarrow \left(\frac{\partial T}{\partial r}\right)_0^0\bigg|_{\mathrm{icb}} r_i^2 = \left(\frac{\partial T}{\partial r}\right)_0^0\bigg|_{\mathrm{cmb}} r_o^2 \tag{26}$$

This allows to formulate a simple relation between the mean radial temperature gradient at the inner and outer boundary.

$$\Leftrightarrow \left(\frac{\partial T}{\partial r}\right)_0^0\bigg|_{\mathrm{icb}} = \left(\frac{\partial T}{\partial r}\right)_0^0\bigg|_{\mathrm{cmb}} \frac{r_o^2}{r_i^2} = -\beta \frac{r_o^2}{r_i^2} = -\beta \frac{1}{a^2} \tag{27}$$

with $\beta := -\left(\frac{\partial T}{\partial r}\right)_0^0\Big|_{\mathrm{cmb}}$ as prescribed temperature gradient at the CMB.
This relation allows us to formulate Neumann boundary conditions for the stationary temperature equation that has the form of a Laplace equation,

$$\nabla^2 T = 0 \tag{28}$$

since there are no internal sources.

$$\text{ICB:} \quad \frac{\partial T}{\partial r}\bigg|_{\mathrm{icb}} = -\beta \frac{1}{a^2} \mathcal{Y}_0^0 \tag{29}$$

$$\text{CMB:} \quad \left.\frac{\partial T}{\partial r}\right|_{\text{cmb}} = -\beta \mathcal{Y}_0^0 + Amp_l^m \mathcal{Y}_l^m \tag{30}$$

where Amp_l^m is the amplitude of the heat flux heterogeneity.
The general solution of (28) in spherical coordinates reads

$$T = \sum_{l,m} \left[a_l^m r^l + b_l^m r^{-l-1}\right] \mathcal{Y}_l^m(\vartheta, \varphi) \tag{31}$$

and its radial derivative

$$\frac{\partial T}{\partial r} = \sum_{l,m} \left[l a_l^m r^{l-1} - (l+1) b_l^m r^{-l-2}\right] \mathcal{Y}_l^m(\vartheta, \varphi). \tag{32}$$

From (29) and (32) follows immediately for $l = m = 0$

$$-b_0^0 r_i^{-2} = -\beta \frac{1}{a^2} \quad \Rightarrow \quad b_0^0 = \beta r_o^2 \tag{33}$$

and the algebraic equation

$$l a_l^m r_i^{l-1} - (l+1) b_l^m r_i^{-l-2} = 0 \tag{34}$$

for all $l > 0$ and $m > 0$.
(30) and (31) together give another equation for the determination of a_l^m and b_l^m:

$$l a_l^m r_o^{l-1} - (l+1) b_l^m r_o^{-l-2} = Amp_l^m. \tag{35}$$

Since only a heat flux pattern with $l = m = 2$ will be used here, (34) and (35) simplify to

$$\begin{pmatrix} 2r_o & -3r_o^{-4} \\ 2r_i & -3r_i^{-4} \end{pmatrix} \begin{pmatrix} a_2^2 \\ b_2^2 \end{pmatrix} = \begin{pmatrix} Amp_2^2 \\ 0 \end{pmatrix}. \tag{36}$$

In a nondimensional form, the solution (28) is

$$\hat{T} = \frac{T}{d\beta} = \left(\frac{a_0^0}{d\beta} + \frac{1}{(a-1)^2 \hat{r}}\right) \mathcal{Y}_0^0 + \frac{Amp_2^2}{\beta} \cdot \frac{2a^5 \hat{r}^3 - 3(a-1)^5 \hat{r}^2}{6(a-1)^4(1-a^5)} \mathcal{Y}_2^2 \tag{37}$$

with a_0^0 being an arbitrary integration constant that is chosen to be 0 in the following.

3 Numerical Method

4 State of research

5 Thermo-chemical core convection

5.1 The formation of stationary vortex columns attached to mantle heterogeneities

6 Thermo-chemical dynamo action

6.1 The creation of radial magnetic flux patches locked to the mantle

6.2 The influence of chemical forcing on magnetic field properties

7 Summary

8 Conclusion and Outlook

References

Blakely, R. J. (1996). *Potential theory in gravity and magnetic applications.* Cambridge University Press.

Kundu, P. and Cohen, I. (2008). Fluid mechanics. *Academic, San Diego.*

Tilgner, A. (2007). *Rotational Dynamics of the Core*, volume 8. cited By 12.